Structural Characteristics and Mechanical Properties of Compositionally Modulated Metallic Multilayers

N.K. Flevaris* and J. Stoemenos
Department of Physics, Aristotle University of Thessaloniki,
540 06, Thessaloniki, Greece

ABSTRACT

Compositionally modulated metallic thin films were prepared by dual-source thermal evaporation with modulation periods containing a small number of atomic planes. The structure of these materials was studied by x-ray diffraction as well as conventional and cross-sectional transmission electron microscopy. It was found that the primary defect type was the twinning which also determined the various growth modes. The latter were observed to be characteristically depended on the extent of the modulation period as was the twinning character, also. Thus, depending on this period, the primary parameter for the structural properties could be either the coherency strains or the chemical modulation, as well as an interplay of the two. This model is considered in discussing the mechanical properties of such materials and especially the so-called "supermodulus effect".

I. Introduction

This contribution concerns structural studies, by electron microscopy, of metallic thin films containing a one dimensional artificial periodicity of the composition. In the rapidly growing field of research on such materials, with both fundamental and technological interests, terms such as compositionally modulated systems, superlattices, multilayers or layered structures have been used often with no distinction in context. Large numbers of works have appeared recently dealing with preparation or properties of such compositionally modulated multilayers [CMM] metallic thin films. For various CMM systems interesting properties have been predicted or observed experimentally. We refer to recent review reports; e.g. for the mechanical properties and the "supermodulus effect" [1] and for preparation, structure and various properties [2-5].

In the theoretical works or the interpretation of experimental studies many different pictures have been assumed or proposed concerning the structure of metallic CMM. Let us outline the principle structural characteristics and complications introduced by the modulation uniquenesses. Ideally, the simplest description of a binary CMM would

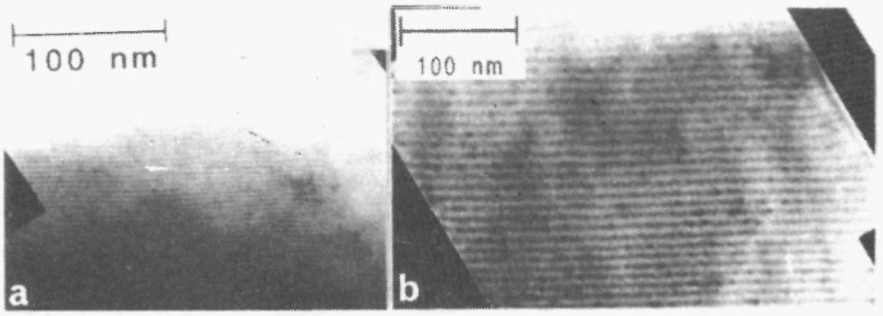

Fig. 1. Typical XTEM micrographs for (a) Cu7-Ni7 and (b) Cu33-Ni22.

then be the CMM with a modulation period (λ) containing m and n atomic planes of A and B, respectively; the notation A_m- B_n will be used to denote such a modulation. However, the following must be considered:

1. The reduced sharpness of the A/B interfaces due to interdiffusion or other sources.
2. The flatness of the layers and the interface due to growth thermodynamical reasons.
3. The crystallinity and defects of the average structure and the interfaces.
4. The degree of coherence between the constituent lattices for crystalline films.
5. The interplanar-spacing modulation (due to coherency strains) superimposed (but not necessarily scaling) with the composition modulation.
6. Both the (concentration and strain) modulation profiles since almost always reality departs from the ideal A-B stacking.

The above characteristics originate from different, thermodynamical or even technical, reasons but they apply to all kinds of metallic CMM as they have been prepared to-date by thermal evaporation (sometimes by

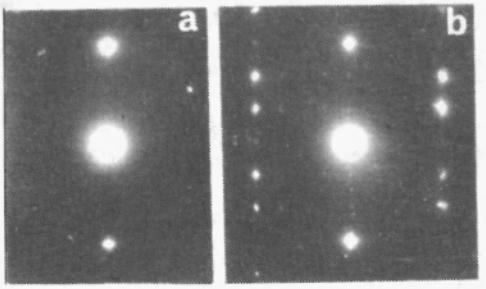

Fig. 2. (a) Typical XTED patterns for CMM. (b) That for its embedded twin.

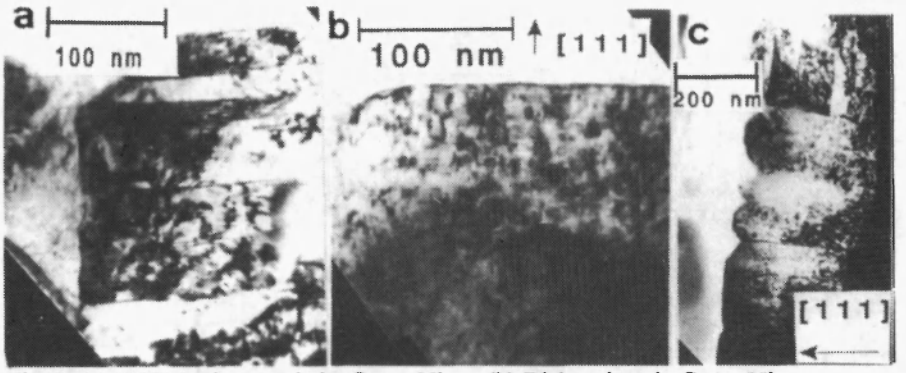

Fig. 3. (a) XTEM micrograph for $Cu_{6.8}$-$Ni_{7.0}$. (b) Dislocations in $Cu_{6.8}$-$Ni_{7.0}$. (c) Extended picture of the growth of the $Cu_{6.8}$-$Ni_{7.0}$ sample.

molecular beam epitaxy) or sputtering. Some works have used the previously mentioned different names for their CMM on the assumption that some of these structural characteristics are being ignored or taken care of by the selection of the constituent elements.

Property investigations have revealed interesting and often unusual behaviour for various CMM metallic systems [1-5]. It has been generally recognised that a structural characterisation is necessary for the evaluation of such studies. Especially for CMM, with fcc constituents, grown on mica there have been mechanical [6-9], magnetic [10-17] and optical [18] property investigations that suggested or explored important modulation, strain or structural influences. Structural studies by x-ray diffraction [5,12,15-17,19-21] or electron microscopy [17,22-29] on such systems have demonstrated the necessity for extensive investigations of the microstructure and the growth mechanisms in order to approach finally a possible assessment of the growth/structure/properties interplay.

In this report we will present our work on the structural studies of two CMM metallic systems Cu-Ni and Pd-Ni, prepared by e-gun thermal evaporation and studies [2,5,8,14,15,17,18] in various property investigations. In section II the experimental techniques used for the film growth and specimen preparation for electron microscopy investigations. The results of (conventional planar) and cross-sectional (CTEM and XTEM, respectively) transmission electron microscopy will be presented and discussed in Section III and, finally, in Section IV we will discuss the possible effects of the structural characteristics on properties and especally the so-called supermodulus effect.

II. Experimental Techniques

A. Growth

The Cu-Ni and Pd-Ni CMM were prepared in a dual e-gun

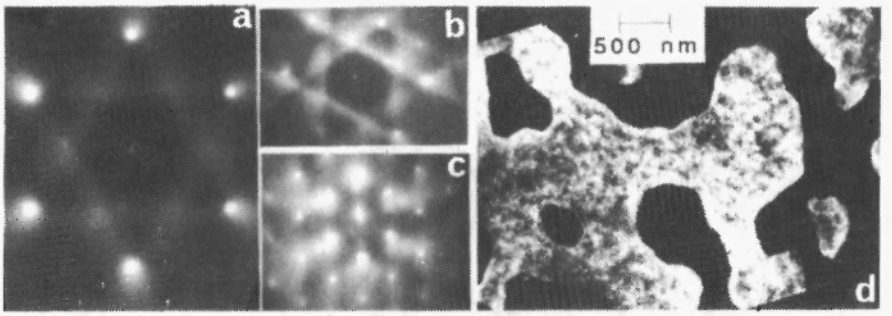

Fig. 4. (a) Typical 111 planar TED for our CMM. (b,c) Corresponding 110 and 114 TED having as common pattern that of (a). (d) Dark-field planar micrograph showing an example of the puzzle-like embedded twin structure.

evaporation unit. The substrate was mica. The substrate temperatures used ranged between 420-600 K for Cu-Ni and 400-550 K for Pd-Ni, depending on the modulation periods that were sought. The fluxes were alternatively interrupted by a reciprocating shutter. The deposition rates ranging between 0.2 and 1 nms^{-1}, were monitored individually by quartz-crystal monitors that allowed steady rates to ~1%.The total thicknesses of the films were about 1 to 2.5 μm for Cu-Ni and 0.1 to 1 μm for Pd-Ni. An oil diffusion pump was employed together with cryopumps; the background vacuum was ~$2\text{-}5\times10^{-7}$ Torr and during deposition ~$1\text{-}5\times10^{-6}$ Torr.

Prior to depositing the CMM a layer of Cu (or Pd) was deposited onto the mica (heated to ~570-620 K) and the temperature was lowered for the deposition of the CMM. The thickness of this buffer layer was 50-75 nm.

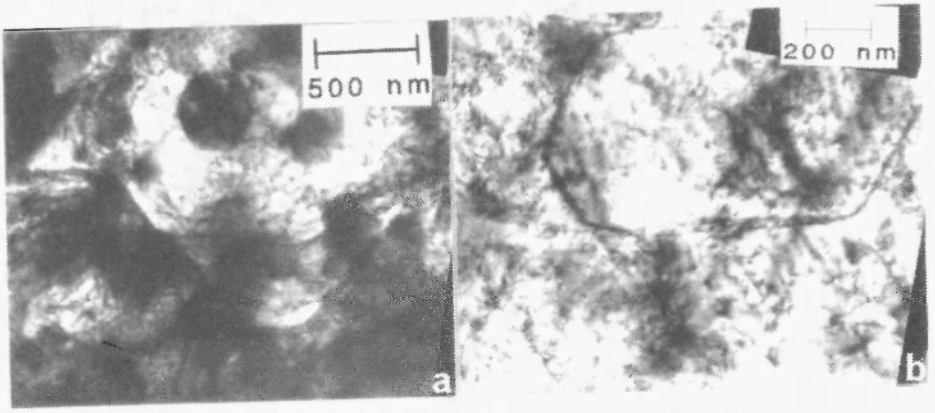

Fig. 5. (a) A hexagonally shaped crystallite and (b) extract of such boundary structure.

B. x-ray characterization

The average structural characteristics were studied routinely by x-ray θ-2θ diffraction.Thus, information was immediately obtained about the

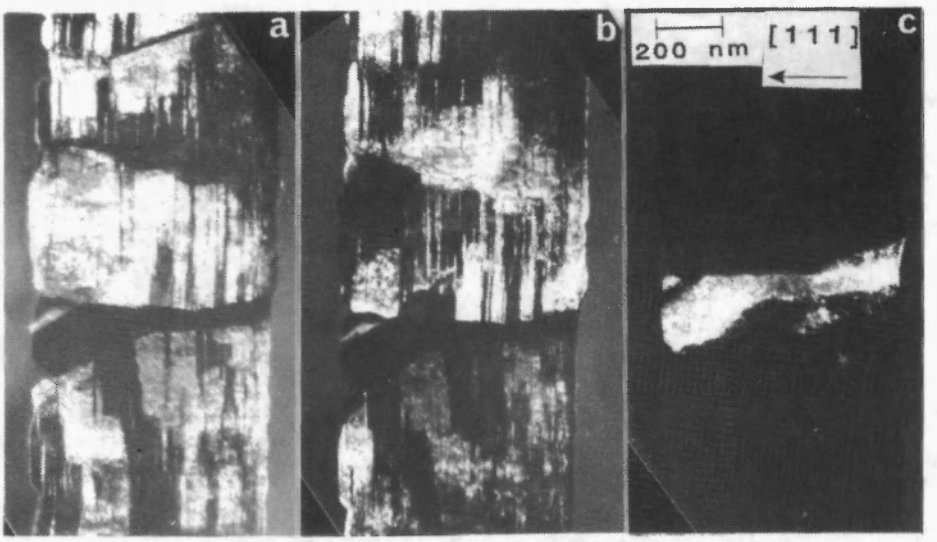

Fig. 6. A study of the embedded and the columnar twin structure in cross-section.

average composition and the λ; for Cu_m-Ni_n these m/(m+n) and λ~m+n values allowed the determination of m and n. It was shown [30] that, for λs containing small m and n, it was possible to prepare Cu-Ni films with very sharp x-ray patterns, when the modulation was commensurate with the individual lattices (i.e. m and n being near integers). This routine x-ray characterisation was used for the calibration of the deposition rates and shutter-reciprocation frequency so that optimisation of the CMM qualities would be achieved as it could be determined by the x-ray modulation-satellite diffractions.

For fcc materials deposited onto heated mica it is known that strong <111> texture will develop and this results in strong "solid solution" diffraction. Around these peaks the satellite diffraction due to the artificial modulation will appear so that the position and intensity of these satellites relative to the central peak may reveal, respectively, extent (λ) and amplitude of the modulation profiles. In principle, for a coherent structure the unknowns will be the numbers m and n, the m+n values of the interplanar spacings within each λ; for a centrosymmetric model this number of unknowns would reduce to its half. The small-angle diffraction (due to composition modulation) and the higher order diffraction (due to both modulations) is not possible to provide enough data that would allow the fitting of all those unknown values. Although a detailed theoretical analysis has been reported [31] and several modelling simplifications have been performed [2,5,32,33] there are still several experimental observations that remain to be addressed while, at present, the basic question of an accurate determination of the modulation profiles is an obvious drawback in the works on CMM.

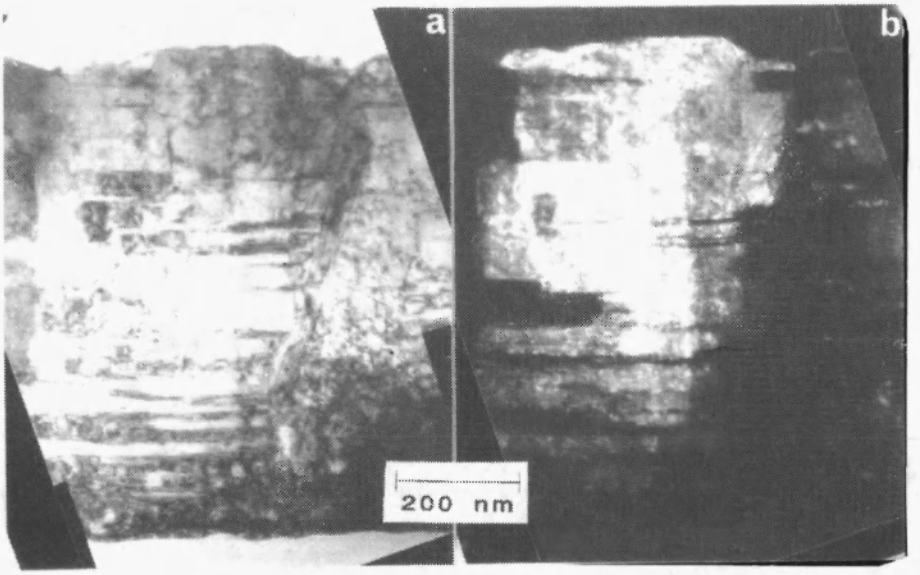

Fig. 7 (a) The shape of the columnar twins and (b) the corresponding dark-field XTEM.

C. Specimen preparation for CTEM and XTEM

First, for CTEM observations the material was removed from mica and were thinned by conventional chemical and ion-beam etching; combinations of the two methods were also used. The observations did not depend on the thinning technique. Second, for XTEM studies a special technique [34] was used. The foil was sandwiched between two Si plates in the form of a narrow strip. This construction was thinned mechanically and with a subsequent ion-beam milling specimens were obtained for edge-on-geometry observations. (The Si plates allowed for the accurate determination of the specimen geometry in the microscope; namely, the <110> of Si was made to coincide with the <111> of the CMM so that all orientation operations had a well established reference.) Transmission electron microscopes operating at 100, 120 and 200 kV were used at different phases of the work. Operation voltages of 20-100 kV were used.

III. Electron Microscopy Observations

The micrographs seen in Fig. 1 depict the thickness profile of two, (a) for Cu_7-Ni_7 and (b) for Cu_{33}-Ni_{22}, samples as observed by XTEM. This picture of CMM approaches that of an ideal multilayer with defect-free stacking of the constituent layers. The modulation is revealed, in Fig. 2, by the satellite spots around the main diffraction. Indeed, as mentioned before for the case of x-ray diffraction, the artificial periodicity λ will

show as extra reflection around the transmitted beam (zeroth-order or small-angle) and the 111 fcc spots. The position of these satellites provided the (m+n) values in agreement with those obtained from x-ray diffraction. From densitographic pictures of such 111 XTED patterns one can estimate the (m+n) values. Unfortunately, it is not possible to extract the quantitative information about the composition and strain analysing such densitographs [35]. We only note the asymmetry in the intensities of the inner ("negative") and outer ("positive") of the 111 satellites in direct correspondence with x-ray diffraction; this was observed for all the Cu_m-Ni_n films CMM films that we studied. Also, it must be noted that the CuNi system would not be the most appropriate one for strong small-angle (i.e. due to composition fluctuations) satellite diffraction since the constituents have similar scattering properties; overfocused exposures are necessary for the study of such diffractions.

Nevertheless, the satellites of the transmitted beam may be an indication of high amplitude of composition modulation and the intensity-asymmetric 111 satellites reveal coherency-strain fields. By including a large number of modulation fringes in micrographs such as in Fig. 1 or by using XTED patterns (and their microdensitographs) we obtained values of λ to compare to those from x-rays. For a more quantitative experiment on the modulation profiles of CMM systems one would need [36] accurate lattice image experiments that could allow the separation of different contributions; however, it must be noted that in the case of lattice imaging of CMM one should be very cautious [37] of the artefacts introduced by the lens aberration effects in phase variations that could result in estimating larger than the actual periodicities.

It would be desired to be able to separate the effects of the displacement and composition fluctuation into the scattered intensity. These difficulties have been assessed recently [38]. However, the effort is still in progress [39] so that Fresnel data, combined with displacement data from the fringe shift, would allow a quantitative analysis of the local compositional fluctuation. In this work we will not be dealing with this problem and confine our interest in the defects of the structure and the growth modes.

The 111 XTED, seen in Fig. 2(a), would be common for a textured (along [111]) fcc thin film. After rotating the edge-on specimen by 30^o around the [111] and bringing one zone axis (i.e. of the <110> or the <112> type) parallel to the e beam it is possible to examine whether the material is monocrystalline or there are, in such a textured specimen, crystallites having a rotational relationship with the matrix. As it will be seen in Fig. 2(b), for a Cu-Ni sample, it is possible to have embedded twins or crystallites in a 30^o relationship as it was also observed for all our Cu_m-Ni_n and Pd_m-Ni_n CMM films. However, as it will be shown later there is a significant difference in the origin of the diffraction seen in Fig. 2(b) for the two systems.

A XTEM micrograph, for a $Cu_{6.8}$-$Ni_{7.0}$ sample, taken with the <110> diffraction indicated in Fig. 2(a) is seen in Fig. 3(a). This

micrograph exhibits the coexistence of high-angle grains and twins in an almost dislocation-free structure. The micrograph seen in Fig. 3(b) indicates the possibility of a dislocated structure, for the same specimen, when the features of Fig. 3(a) are absent. The overall edge-on structure of this $Cu_{6.8}$-$Ni_{7.0}$ sample is shown in Fig. 3(c) where one can see: a) A columnar growth mode with average in-plane column extent of about 100-500 nm. b) A tooth-like surface morphology. c) Columnar grains with extensive twining. d) Columnar grains with threading dislocations. Finally, in combination with the higher resolution micrograph of Fig. 3(a) we can note: e) The crystallographic sharpness of the (111) twin boundaries. f) The existence of "inclined" modulation fringe sequences. g) The interpenetration of modulation fringes and twin boundaries without evident distortion of either the two. In the following we will examine further these points for samples with various m and n via CTEM and XTEM investigations.

A conventional planar transmission electron diffraction (TED), commonly observed for our Cu_m-Ni_n samples, is seen in Fig. 4(a) which is obtained with the electron beam along the [111] and corresponds to the average structure of the CMM. The TED patterns seen in Fig. 4(b,c) will show how differently oriented crystallites with a twin relationship had the common TED of Fig. 4(a). The [110] zone-axis pattern and its twin with the [114] zone axis seen in Figs. 4 (b) and (c), respectively, obtained with the film normal rotated by 35^o around the [110] of the film plane, reveal the existence of twin crystallites. When a non-common 111 reflection of Fig. 4(b) is excited one can see the diffracted domains in the dark-field CTEM micrograph seen in Fig. 4(d). Similar structure was observed for various Cu_m-Ni_n films with its major feature being the doubly positioned twin crystallites which formed this labyrinthic ("puzzle-like") crystals extending over several micrometers in the film plane. Each crystal contained microtwins in varying but low densities, regularly shaped crystallites and their twin boundaries would be coherent or incoherent. Such a crystallite is shown in Fig. 5(a) with a hexagonal shape. It is evident that this crystallite has been isolated as a column in a larger crystal which is a twin of the surrounding matrix as well as this particular crystallite. This incoherent such twin boundaries were observed to contain steps of small extent that were comprised by (111) and (112)-type faces.

Such boundaries are seen in Fig. 5(b) for a columnar twin in the matrix. The twin boundaries are observed to have a limited width due to their stepped form. The profile of these embedded twins will be depicted in the XTEM investigations to follow. In Fig. 6 we observe edge-on dark-field micrographs for a $Cu_{6.8}$-$Ni_{7.0}$ sample together with the corresponding XTED patterns on which the arrows indicate the diffraction used for each micrograph. Thus, it is evident that the growth of this CMM favoured the formation of embedded twining of the 111 type (Figs. 6(a,b)), columnar twining of the type of Fig. 6(c) while one isolated case of 110 type twining is observed in Fig. 6(a). The first type of those twins

was seen in Fig. 3(a) for which case we note again the observation of "inclined"modulation fringes intercrossing the (111) coherent twin planes without any structural distortion. The crystallographic orientation is shown on the micrograph of Fig. 7(a) while the corresponding dark-field micrograph of Fig. 7(b) depicts the shape of a columnar twinned crystallite. One observation made over many Cu_m-Ni_n CMM is the increase of the embedded twin density and thickness as the total thickness of the foil was increased. There is, however, an important question concerning the effects of the initially grown Cu-buffer layer on the overall structure of the CMM. As seen in Fig. 7, the Cu layer (of about 50nm thickness) was not grown perfectly flat on the mica surface. The buffer layer could be twinned in which case the CMM could also follow in the same type of twinning while when no twinning is observed in the Cu-layer the twinned CMM structure may begin its formation at any thickness. Confirmation of the doubly embedded matrix-twin sequence mentioned in presenting Fig. 5(a) is observed at various points in these XTEM micrographs of Figs. 6-7. Similar observations were made for a variety of Cu_m-Ni_n samples with λs lower than about 6 nm.

IV. Discussion

From the structural properties presented in the previous Section one can deduce the following concerning the structural defects and growth modes. The primary defect is the embedded twinning. However, this is observed to depend on the period λ and one could distinguish three such regimes. For short-λ modulations the coherency strains play the most important role and the interplanar-spacing modulation characterises the overall CMM structure. As λ increases, the role of the chemical modulation is enhanced until it becomes the primary one for very long λs, longer than a critical one, λ_c. As a result, the structure will be dominated by the double-positioning embedded twins for very short λs while growth twins will define the "average" (solid solution) lattice in the case of $\lambda > \lambda_c$. Finally, the twinning process may be defined as an interplay of the above two mechanisms for modulations with intermediate λs. (The value of the critical λ_c for each CMM system, depends on the lattice properties as well as the elastic properties of the constituents.)

The supermodulus effect was, for such CMM systems, has shown that a biaxial elastic modulus depends non-monotonically on λ and a maximum enhancement is observed for λ being around 1.5 - 2.5 nm, for different CMM [3,6-9]; we just note here that it is for this regime of λs that changes occur in the balance of the importance between the short-λ (strain) effect and the intermediate-λ effects where interplay of the two modulations begins. (However, no supermodulus effect, or simply no such enhancement, was observed [7] in the case of Cu-Au grown with 100 texture nor for other CMM systems with no well defined 111 texture while the corresponding well textured CMMs exhibited the supermodulus

effect.) The twinning mechanism as a means for modification of the mechanical and elastic properties is well known. In our case the double-positioning twinning may be considered as the primary mechanism for modifying the coherence of the CMM structure. That is why metallic CMMs are found to be coherent for λ longer than those predicted by the continuum elasticity coherency strain theory. Hence, the biaxial elastic modulus modifications (and enhancement) may be the result of the λ-dependent twinned structural modifications; accordingly, it would be reasonably explained why these effects are absent in poorly textured CMM systems as well as in the case of 100 Cu-Au which, as it is well known, exhibits special structural properties. Finally, one equally important outcome of these structural modifications is the symmetry-breaking or symmetry-lowering for the new CMM structures. Such processes have their signature in various anisotropies.

Acknowledgement: We are indebted to Prof. Th. Karakostas for collaborating in the electron microscopy work. This work was supported by the EEC through a contract in the BRITE / EURAM Action.

References

1. R.C. Cammarata, *Scripta Metall.* 20, 479 (1986).
2. B.C. Giessen et al. (eds.), "*Synthetic Modulated Structures*", Academic, New York (1985).
3. T. Tsakalakos (ed.), "*Modulated Structure Materials*", Martinus Nijhoff, Dordrecht (1984).
4. I.K. Shuller in: "*Physics, Fabrication and Applications of Multilayered Structures*", P. Dhez and C. Weisbuch (eds.), to be published.
5. B.Y. Jin and J.B. Ketterson, *Adv. in Phys.* 38, 189 (1989).
6. W.M.C. Yang, T. Tsakalakos and J.E. Hilliard, *J. Appl. Phys.* **48**, 876 (1977).
7. G.E. Henein, Ph.D. thesis, Northwestern Univ., Evanston, USA (1980)
8. D. Baral, Ph.D. thesis, Northwestern Univ., Evanston, USA (1983).
9. L.R. Testardi, R.H. Willens, J.T. Krause, D.B. McWhan and S. Nakahara, *J. Appl. Phys.* 52, 510 (1981).
10. E.M. Gyorgy, J.F. Dillon, D.B. McWhan, L.W. Rupp Jr., L.R. Testardi and P.J. Flanders, *Phys. Rev. Lett.* 45, 57 (1980).
11. J.Q. Zheng, C.M. Falco, J.B. Ketterson and I.K. Schuller, *Appl. Phys. Lett.* 38, 424 (1981).
12. E.M. Gyorgy, D.B. McWhan, J.F. Dillon, Jr., L.R. Walker and J.V. Waszcak, *Phys. Rev.* B25, 6739 (1982).
13. G.P. Felcher, *J. Magn. Magn. Mat.* 21, L198 (1980).
14. N.K. Flevaris, J.B. Ketterson and J.E.Hilliard, *J. Appl. Phys.* 53, 8046 (1982).
15. N.K. Flevaris,J.B. Ketterson and J.E.Hilliard, *J. Appl. Phys.*, 53, 2439 (1982).
16. H. Sakakima, R. Krishnan and M. Tessier, *J. Appl. Phys.* 57, 3651 (1985).
17. N.K. Flevaris, M. Porte and R. Krishnan, *J. de Physique* C8, 1771 (1988).
18. N.K. Flevaris and S. Logothetidis, *Appl. Phys. Lett.* 50, 1544 (1987).
19. I.K. Schuller, *Phys. Rev. Lett.* 44,1597 (1980).
20. W.P. Lowe, T.W. Barbee,Jr., T.H. Geballe and D.B. McWhan, *Phys. Rev.* B24, 6193 (1981).

21. N. Sato, *J. Appl. Phys.* 64, 6424 (1988).
22. A. Purdes, *Ph.D. Thesis* (unpublished), Northwestern University, Evanston USA (1976).
23. S. Nakahara, R.J. Schutz and L.R. Testardi, *Thin Solid Films* 72, 277 (1980).
24. C.S. Baxter and W.M. Stobbs, *Appl. Phys Lett.* 48, 1202 (1986).
25. Th. Karakostas and N.K. Flevaris, *J. Mater Sci. Lett.* 5, 1235 (1986).
26. R.E. Somekh, W.C. Shin, K. Dyrbye, K.H. Huang and C.S. Baxter, *SPIE Proc. X-Ray Instrumentation* 453, 1140 (1989).
27. N.K. Flevaris and Th. Karakostas, *J. Appl. Phys.* 63, 1228 (1988).
28. N.K. Flevaris and Th. Karakostas in: "*Alloy Phase Stability*", G.M. Stocks and A. Gonis (eds.), Kluwer Academic Publs., Dordrecht (1989), p. 591.
29. C.S. Baxter and W.M. Stobbs, *Ultramicrosc.* 16, 213 (1985).
30. N.K. Flevaris, D. Baral, J.E. Hilliard and J.B. Ketterson, *Appl. Phys. Lett.* 38, 992 (1981).
31. D. de Fontaine in: "*Local atomic Arrangements Studied by x-ray Diffraction*", J.B. Cohen and J.E. Hilliard (eds.), Gordon and Breach, New York (1966).
32. A. Segmuller and A.E. Blakeslee, *J. Appl. Cryst.* 6, 19 (1973); ibid 6, 413 (1973).
33. D.B. McWhan, M. Gurvitch, J.M. Powell and L.R. Walker, *J. Appl. Phys.* 54, 3886 (1983).
34. M. Dupuy, *J. Microsc. Spectrosc. Elect.* 9, 163 (1984).
35. R. Sinclair and G. Thomas, *Metall. Trans.* A9, 373 (1978).
36. C.K. Wu, R. Sinclair and G. Thomas, *Metall Trans.* A9, 381 (1978).
37. J.C.A. Spence, J.M. Cowley and R. Gronsky, *Ultramicrosc.* 4, 429 (1979).
38. J.M. Vitek, *Ultramicrosc.* 22, 197 (1987).
39. W.M. Stobbs, *J. de Phys.* C5, 48, 33 (1987).